Competing Crystal Phases in the Lowest Landau Level

Alexander C. Archer,[1] Kwon Park,[2] and Jainendra K. Jain[1]

[1]*Department of Physics, 104 Davey Lab, The Pennsylvania State University, University Park, Pennsylvania 16802, USA*
[2]*School of Physics, Korea Institute for Advanced Study, Seoul 130-722, Korea*

(Received 21 June 2013; published 2 October 2013)

We show that the solid phase between the 1/5 and 2/9 fractional quantum Hall states arises from an extremely delicate interplay between type-1 and type-2 composite fermion crystals, clearly demonstrating its nontrivial, strongly correlated character. We also compute the phase diagram of various crystals occurring over a wide range of filling factors and demonstrate that the elastic constants exhibit nonmonotonic behavior as a function of the filling factor, possibly leading to distinctive experimental signatures that can help mark the phase boundaries separating different kinds of crystals.

DOI: 10.1103/PhysRevLett.111.146804 PACS numbers: 73.43.−f, 71.10.Pm

A Wigner crystal (WC) [1] is expected to form when the interaction energy of electrons dominates their kinetic energy. One way to accomplish this is to force all electrons in two dimensions into the lowest Landau level (LL) by applying a large magnetic field [2]. The insulating phase at filling factors $\nu < 1/6$ has been interpreted in terms of such a crystal [3–11], although a definitive observation of the crystalline order is so far lacking. Remarkably, an insulating phase also appears between the fractional-quantum-Hall-effect (FQHE) [12] liquids at $\nu = 2/9$ and $1/5$ [3–5]. The facts that this insulator has persisted even as the sample mobility has risen tenfold and that it is flanked by two FQHE liquids suggest that the insulating behavior is probably caused by pinning of a crystal rather than individual carrier freeze-out. While a qualitative scenario for the reentrant behavior can be constructed in terms of cusps in the energy of the liquid state [3], this behavior so far has not been explained by a quantitative theoretical calculation. We show in this Letter that this insulating state results from an extremely subtle competition between the crystal and liquid states. Our results support the interpretation of this insulator as a pinned crystal, while also demonstrating its nontrivial nature as a crystal of composite fermions (CFs). We also consider the phase diagram of the crystal phase in a wider range of filling factors, calculate the elastic constants, and predict their nonmonotonic behavior as a function of ν.

Numerous theoretical studies have considered the crystal phase [13–27]. Maki and Zotos (MZ) [13] considered an uncorrelated Hartree-Fock WC of electrons in the lowest LL and evaluated its elastic properties. Lam and Girvin (LG) [14] considered a correlated WC, the energy of which has been compared [14,28] with those of $1/m$ [29] and $n/(2pn+1)$ FQHE states [30] (m odd integer; n, p integers), which shows a level crossing transition at $\nu \approx 1/6$. Beginning with Yi and Fertig [18], a number of studies considered crystals of composite fermions [19,22–24,26,27]. In particular, Chang *et al.* [24] demonstrated that the CF crystals (CFCs) accurately capture the correlations in the crystal phase.

For the questions addressed in this work, we need the energies of both the crystal and the FQHE states as a *continuous* function of ν. For this purpose, we will consider two types of CFCs. Denoting composite fermions carrying $2p$ vortices by ^{2p}CFs, these are the following. (i) "Type-1 ^{2p}CFC" refers to a state in which *all* ^{2p}CFs form a crystal. When pinned by disorder, this state will exhibit insulating behavior with divergent longitudinal resistance. (ii) The term "type-2 ^{2p}CFC" refers to a state in which the excess CF particles or holes [31] relative to a FQHE liquid form a crystal. A type-2 CFC rides on the background of a FQHE liquid. In the presence of some disorder that pins the type-2 CFC, this state exhibits quantized Hall resistance and dissipationless transport. Type-2 CFCs, which can be likened to a pinned Abrikosov vortex lattice in a type-2 superconductor, are unobservable in transport experiments but can be detected in microwave resonance experiments [32] or by direct measurement of the spatial density profile (shown below for some cases).

We will consider N electrons on the surface of a sphere exposed to a total flux $2Q$ in units of hc/e. This geometry [33] is convenient for its lack of boundaries and obviates the complications requiring the introduction of "ghost charges" [18]. We will denote the electron coordinates on the sphere as $\boldsymbol{r}_j = (\theta_j, \phi_j)$, $j = 1, \ldots, N$, and the crystal sites by $\boldsymbol{R}_l = (\gamma_l, \delta_l)$, with $l = 1, \ldots, N_c$, where N_c is the number of lattice sites. It is also convenient to define the spinor variables $(u, v) = (\cos(\theta/2)e^{i\phi/2}, \sin(\theta/2)e^{-i\phi/2})$ and $(U, V) = (\cos(\gamma/2)e^{i\delta/2}, \sin(\gamma/2)e^{-i\delta/2})$. A problem with this geometry is that it is not possible to tile the surface of a sphere with a crystal without introducing defects. We place the crystal wave packet centers at the locations that minimize the energy of charged point particles on the surface of a sphere. Finding these locations, widely known as the Thomson problem [34], has been accomplished previously by a number of researchers using powerful numerical techniques [35]. The Thomson crystal is locally a triangular WC, and the fraction of defects vanishes as $N_c \to \infty$.

We construct explicit wave functions as follows. The system of electrons at $2Q$ maps into a system of composite fermions at $2Q^* = 2Q - 2p(N-1)$ [30]. We first construct $\Phi^{\text{type-}K\text{-MZ}}_{2Q^*,\{\boldsymbol{R}\}}$, namely, the type-$K$ uncorrelated MZ crystal at $2Q^*$ in which N_c particles are located at the Thomson positions $\{\boldsymbol{R}_1, \ldots, \boldsymbol{R}_{N_c}\}$. We then obtain the type-K ^{2p}CFC according to the mapping

$$\Psi^{\text{type-}K\text{-CFC}}_{2Q,\{\boldsymbol{R}\}} = \mathcal{P}_{\text{LLL}} \prod_{j<k} (u_j v_k - v_j u_k)^{2p} \Phi^{\text{type-}K\text{-MZ}}_{2Q^*,\{\boldsymbol{R}\}}, \quad (1)$$

where the Jastrow factor $\prod_{j<k=1}^{N}(u_j v_k - v_j u_k)^{2p}$ attaches $2p$ vortices to electrons and $\mathcal{P}_{\text{LLL}}$ is the lowest LL projection operator, which will be evaluated by the Jain-Kamilla method [28]. Under this mapping, electrons, LLs, and MZ crystals get converted into CFs, ΛLs, and CFCs, respectively. For the type-1 ^{2p}CFC, we have $N_c = N$ and the allowed $2p$ values are such that $N < 2Q^* + 1$; here,

$$\Phi^{\text{type-1-MZ}}_{2Q^*,\{\boldsymbol{R}\}} = \det \phi^{2Q^*}_{\boldsymbol{R}_l}(\boldsymbol{r}_j) = \det(U_l^* u_j + V_l^* v_j)^{2Q^*}, \quad (2)$$

where $\phi^{2Q^*}_{\boldsymbol{R}}(\boldsymbol{r}) = (U^* u + V^* v)^{2Q^*}$ is the maximally localized wave packet in the lowest LL. For the type-2 ^{2p}CFC, there are two possibilities. For certain values of $2Q^*$ we have $n \geq 1$ filled LLs and N_c particles in the $(n+1)$th partially filled LL. For convenience of illustration, let us take $n = 1$, which corresponds to the FQHE state in the range $2/(4p+1) > \nu > 1/(2p+1)$. The wave function of the MZ crystal is given by

$$\Phi^{\text{type-2-MZ}}_{2Q^*,\{\boldsymbol{R}\}} = \begin{vmatrix} Y_{Q^*Q^*-Q^*}(\boldsymbol{r}_1) & \ldots & Y_{Q^*Q^*-Q^*}(\boldsymbol{r}_N) \\ \vdots & \ddots & \vdots \\ Y_{Q^*Q^*Q^*}(\boldsymbol{r}_1) & \ldots & Y_{Q^*Q^*Q^*}(\boldsymbol{r}_N) \\ \mathcal{O}^\dagger \phi^{2(Q^*+1)}_{\boldsymbol{R}_1}(\boldsymbol{r}_1) & \ldots & \mathcal{O}^\dagger \phi^{2(Q^*+1)}_{\boldsymbol{R}_1}(\boldsymbol{r}_N) \\ \vdots & \ddots & \vdots \\ \mathcal{O}^\dagger \phi^{2(Q^*+1)}_{\boldsymbol{R}_{N_c}}(\boldsymbol{r}_1) & \ldots & \mathcal{O}^\dagger \phi^{2(Q^*+1)}_{\boldsymbol{R}_{N_c}}(\boldsymbol{r}_N) \end{vmatrix}, \quad (3)$$

where $Y_{QQm}(\boldsymbol{r}) \propto (-1)^{Q-m} v^{Q-m} u^{Q+m}$ are the lowest LL monopole harmonics [31], $N_c = N - (2Q^* + 1)$, and $\mathcal{O}^\dagger = v^*(\partial/\partial u) - u^*(\partial/\partial v)$ is the LL raising operator in the spherical geometry [36] (which also lowers the monopole strength by one unit). For $\nu < 1/(2p+1)$, we form a crystal of $N_c = 2Q^* + 1 - N$ CF holes in the background of one filled Λ level. Here the MZ crystal is obtained by taking the filled LL wave function $\prod_{j<k=1}^{2Q^*+1}(u_j v_k - v_j u_k)$ and replacing the N_c coordinates (u_j, v_j) with $j = N+1, \ldots, 2Q^*+1$ by the Thomson positions (U_l, V_l). $\mathcal{P}_{\text{LLL}}$ is not required for either the type-2 CF-hole crystal or the type-1 CFC.

Figure 1 shows the electron density profiles for various possible crystals for a filling factor slightly larger than 1/5: 1(a) type-1 MZ crystal, 1(b) type-1 ^{2}CFC, and 1(c) and 1(d) type-2 ^{4}CFC. Correlations in the type-1 ^{2}CFC result in a slight delocalization of the electrons at the lattice sites as compared to the MZ crystal [compare Figs. 1(a) and 1(b)]. The type-2 CFC looks remarkably different. An isolated CF in the second Λ level is known to have the shape of a ring [31]. A "ring crystal" is clearly seen in Fig. 1(d) where the composite fermions in the second ΛL are far from one another. The lattice spacing decreases with increasing filling factor, and the rings begin to overlap, producing a complex interference pattern as seen in Fig. 1(c), in which the density maximum occurs on the line joining adjacent sites producing a "bond crystal." Even more intricate density profiles can occur for type-2 CFCs in higher ΛLs.

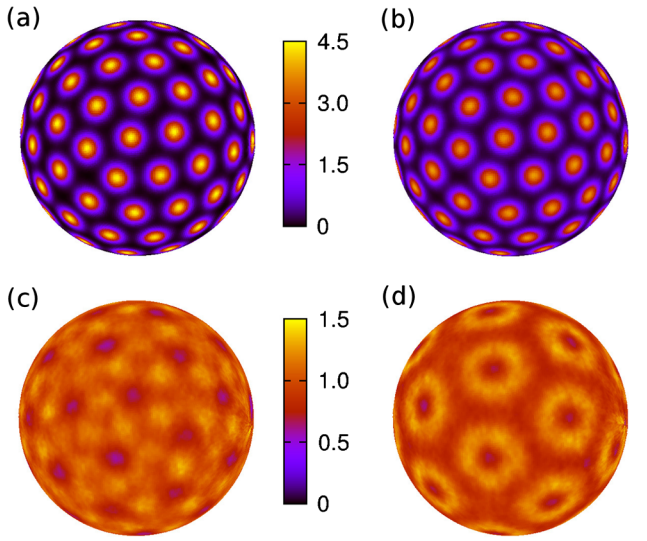

FIG. 1 (color online). Density profiles for some type-1 and type-2 CF crystals on the surface of a sphere. All systems contain $N = 96$ particles. The parameters are (a) MZ crystal and (b) type-1 ^{2}CFC for $2Q = 433$ at $\nu = 0.2188$, (c) type-2 ^{4}CFC for $N_c = 42$ and $2Q = 433$ at $\nu = 0.2188$, (d) type-2 ^{4}CFC for $N_c = 24$ and $2Q = 451$ at $\nu = 0.2103$. The filling factor in this region is determined using the interpolation relation $\nu = (N+2)/(2Q+15)$, which correctly reproduces the known finite size "shifts" in $2Q$ at $\nu = 1/5$ and $\nu = 2/9$. The density is plotted in units of $\rho_0 = N/4\pi R^2$. While comparing different plots, note that the radius of the sphere is $R = \sqrt{Q}$ in units of the magnetic length.

Figure 2 shows the energies, obtained via standard Metropolis Monte Carlo techniques [31], for several type-1 and type-2 CFCs (the latter labeled FQHE) for 96 particles as a function of ν. A reentrant insulating phase appears in a filling factor range between the 1/5 and 2/9 FQHE states, where the type-1 CFC beats the FQHE state (supporting a type-2 CFC) by an energy of 0.0005 $e^2/\epsilon\ell$ per particle. To put this in perspective, we recall that the theoretical excitation gaps at 1/3 and 1/5 are $\sim 0.1 e^2/\epsilon\ell$ and $\sim 0.025 e^2/\epsilon\ell$, respectively. The MZ crystal does not produce the reentrant crystal phase; in spite of apparently small differences in the density profiles, the energy of the MZ crystal is higher by $\sim 0.006 e^2/\epsilon\ell$ per particle than the

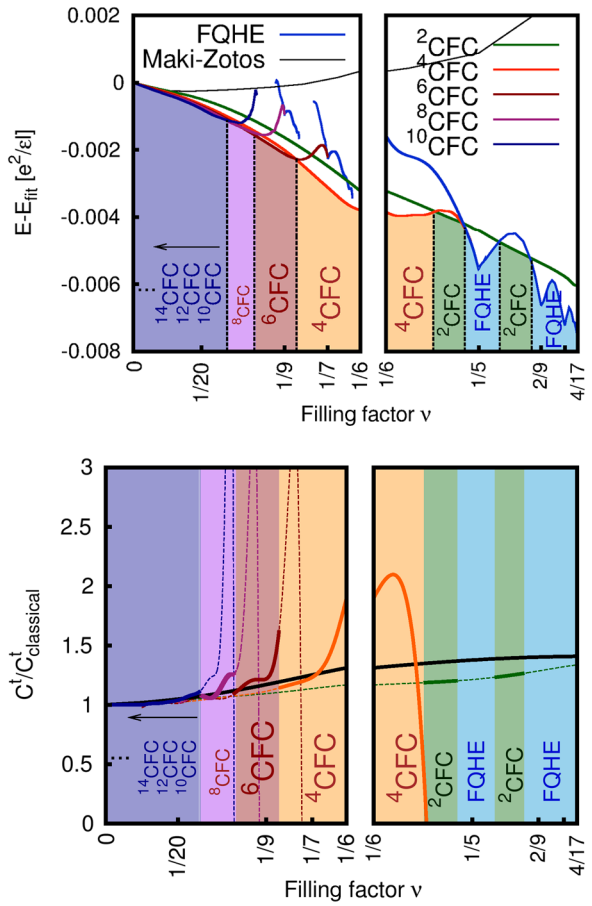

FIG. 2 (color online). Upper panels: Energy per particle as a function of filling factor for various type-1 and type-2 CFC states. The latter are labeled FQHE. All energies are quoted relative to a reference energy $E_{\rm fit} = -0.782\,133\nu^{1/2} + 0.2623\nu^{3/2} + 0.18\nu^{5/2} - 15.1e^{-2.07/\nu}$, which has a form similar to that in Ref. [14] but with coefficients modified to display the energy differences between the competing states more clearly. Lower panels: Shear moduli of type-1 crystals of composite fermions with $2p$ vortices. The shear modulus of the MZ crystal, given by the solid black line, is shown for reference. The shear modulus of the ^{2p}CFC is indicated by a solid line in the regime where it is the ground state and by a dashed line otherwise. The regions $0 < \nu < 1/6$ and $1/6 < \nu < 4/17$ are shown in separate panels because different filling factor scales are used for them.

energy of the type-1 CFC at $\nu \approx 1/5$. The energy of the LG crystal is $0.002\,14e^2/\epsilon\ell$ above the $1/5$ FQHE state and $0.003\,05e^2/\epsilon\ell$ above the $2/9$ FQHE state (using the thermodynamic limits from Refs. [14,28]), and will also not capture the insulating crystal phase between $1/5$ and $2/9$. The understanding of the insulating phase between $1/5$ and $2/9$ as the ^{2}CF crystal leads to the intuitively pleasing picture in which the ^{4}CFs of the nearby liquid states shed two of their vortices to establish a crystal, while retaining energetically favorable correlations through the remaining two vortices.

It has recently been demonstrated [37] that the density distribution of the electrons can be accessed through NMR measurements, because the Knight shift is proportional to the local electron density. As shown in the Supplemental Material [38], the type-1 and type-2 CFCs have remarkably different density distributions, which may allow NMR to identify the phase boundaries in the region $1/5 < \nu < 2/9$.

We have also studied the competition between the liquid and crystal phases at lower fillings, where we consider type-1 ^{2p}CFCs with different choices of $2p$ to determine which produces the lowest energy. As ν is lowered below $1/5$, a series of type-1 ^{2p}CFCs with increasing vorticity occurs. No FQHE state supporting a type-2 CFC appears for $\nu < 1/6$ (We cannot rule out FQHE states with fillings $n/(6n-1)$ in the range $1/5 > \nu > 1/6$, not studied here due to complications associated with reverse flux attachment [39]). The phase boundaries practically remain unchanged for $N > 32$ (see Supplemental Material [38]), and thus represent the thermodynamic limit. We have also studied the effect of finite thickness, which does not change the phase diagram appreciably. Using the model of Ref. [40], we have considered quantum well structures with the well widths ranging from 20 to 80 nm and the electron density ranging from 1.0×10^{10} to 1.5×10^{11} cm^{-2}, and found that even though the energy per particle decreases by up to 10% for the largest densities and widths considered, the phase boundaries are little changed.

To formulate the low-energy dynamics of type-1 CFCs, we begin by modeling the CFC as a collection of charged point particles that interact through an effective interaction $V(R_{jk})$ with $R_{jk} = |\boldsymbol{R}_j - \boldsymbol{R}_k|$, but are otherwise classical. The dynamical matrix $\Phi_{\alpha\beta}(\boldsymbol{k})$, where α, β denote spatial directions, is given by [13]

$$\Phi_{\alpha\beta}(\boldsymbol{k}) = \sum_j [1 - \cos(\boldsymbol{k}\cdot\boldsymbol{R}_j)]\frac{\partial^2 V(R_j)}{\partial R_{j,\alpha}\partial R_{j,\beta}} \simeq \left[\frac{\nu}{k} + (C^L - C^t)\right]k_\alpha k_\beta + \delta_{\alpha\beta}C^t k^2, \quad (4)$$

where $R_j = |\boldsymbol{R}_j|$. In the above, the second line is obtained in the $k \to 0$ limit under the explicit assumption of the C_6 symmetry. Between the two elastic parameters, C^L and C^t, the shear modulus C^t is of special importance because it determines the low-energy behavior of the magnetophonon mode and its becoming negative signals an instability of the crystal. As shown in the Supplemental Material, for the hexagonal lattice it can be obtained directly from the energy per particle of the crystal by the following equation:

$$C^t_{\rm CF} = \frac{1}{2}\nu^2\frac{\partial^2}{\partial\nu^2}(E_{\rm CF} - E_{\rm MZ}) + C^t_{\rm MZ}, \quad (5)$$

where $E_{\rm MZ}$ is defined as the energy of a hexagonal crystal of *classical* particles interacting with the MZ interaction $V_{\rm MZ} = (\sqrt{\pi}/4)(I_0(R^2/8)/\cosh(R^2/8))$, and the derivatives with respect to ν are to be evaluated at fixed B (i.e., fixed ℓ). The derivation of this relation relies on the

assumptions that the dynamics of the crystal can be described in the harmonic approximation and that the total energy can be approximated as a sum of two-body interactions. The latter approximation becomes unreliable as the system approaches $\nu^* = 1$, or $\nu = 1/(2p+1)$, where the crystal wave function actually merges into a FQHE liquid (this is analogous to the fact that at $\nu = 1$ the MZ wave function describes the $\nu = 1$ liquid state). However, for the MZ wave function, this assumption is quite accurate for $\nu < 1/2$ (see Supplemental Material [38]), and by analogy, we expect it to be accurate for ^{2p}CFC for up to $\nu^* < 1/2$, or $\nu < 1/(2p+2)$.

The lower panel of Fig. 2 shows the shear modulus of the ^{2p}CFCs as a function of filling factor. As noted above, the shear modulus for ^{2p}CFC close to $\nu = 1/(2p+1)$ is quantitatively unreliable due to the importance of the three- and higher-body terms in the effective interaction that have been neglected above. Fortunately, in the physically relevant regions, we have $\nu^* < 1/2$, and therefore we believe that $C^t_{\rm CF}$ shown by the solid lines is accurate; the only exception is for ^{4}CFC for which the $C^t_{\rm CF}$ for $\nu > 1/6$ is not quantitatively reliable. The shear modulus exhibits, unlike for the MZ or LG crystal, a series of discontinuities at the phase boundaries, which serve as a possible way of measuring the phase diagram.

Transport [3–5] and photoluminescence [41–43] experiments have probed the temperature dependence of the insulating phase. The melting of the crystal is of interest, and two possibilities can result in remarkably different experimental manifestations. The Kosterlitz-Thouless (KT) [44,45] melting temperature is given by [13] $k_B T_{\rm KT}/(e^2/\epsilon\ell) = (2\pi\sqrt{3})^{-1}(C^t_{\rm CF}/C^t_{\rm classical})0.097\,75\nu^{1/2}$, where $C^t_{\rm classical} = 0.097\,75\nu^{1/2}$. Another possibility is that of melting into the FQHE liquid, considered by Price *et al.* [46], the transition temperature T_M for which is determined by the competition of the free energies of the crystal and liquid states [38]. The resulting transition temperatures are shown in Fig. 3. We find that at $\nu = 1/7$ (and also lower fillings) the transition occurs into a FQHE liquid, whereas for the crystal between $1/5 < \nu < 2/9$ the melting is governed by the KT physics; the difference arises because of much larger roton gap at $1/5$. The inset shows the phase boundary as a function of the filling in the range $1/5 < \nu < 2/9$. Note that, for a narrow range of ν, the FQHE state freezes into a type-1 CFC with increasing temperature and then melts back into the FQHE state; the possibility of a similar reentrant transition was noted previously in Ref. [46] at $\nu = 1/3$ and $1/5$ at certain values of LL mixing.

Chitra *et al.* [47,48] have developed an elastic model which predicts the pinning frequency of the classical WC. Using the shear moduli of the type-1 ^{2p}CFCs, we find nontrivial quantum corrections to the classical pinning frequencies. The magnetic field dependence of the pinning frequency has two forms depending on the length scale of disorder, r_f: $\omega_p \propto \nu/C^t_{\rm CF}$ for $r_f > \ell$ and $\omega_p \propto (\nu^2 C^t_{\rm CF})^{-1}$ for $r_f < \ell$, assuming constant density. Clearly, the discontinuity of the $C^t_{\rm CF}$ at the phase boundaries will translate into a discontinuity in ω_p.

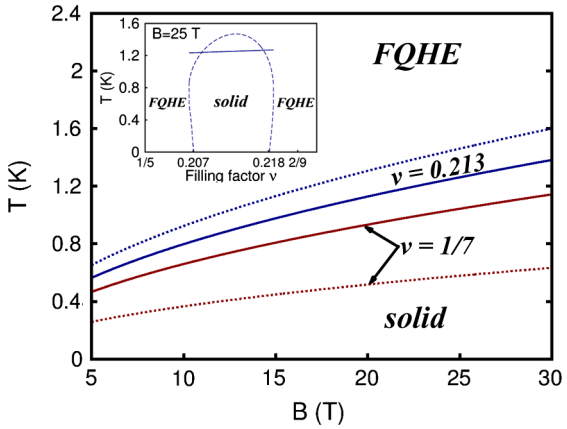

FIG. 3 (color online). Melting temperature of the CF crystal at $\nu = 1/7$ and $\nu = 0.213$ as determined by the Kosterlitz-Thouless mechanism (solid lines) and a first order transition into a FQHE liquid [46] (dotted lines). The inset shows the phase diagram in the filling factor range $1/5 \le \nu \le 2/9$ for $B = 25$ T.

Several features of our calculation are consistent with experimental observations. The range of the reentrant crystal in Fig. 2, $0.207 < \nu < 0.218$, agrees with the region where activated behavior has been observed [3]. No type-1 ^{2p}CFC appears for $\nu > 2/9$, consistent with an absence of an insulator here in high quality samples. The observation of FQHE-like structure at very low fillings (such as $1/7$ and $1/9$) observed in Ref. [5] at somewhat elevated temperatures is consistent with a melting of the crystal into a FQHE state. The frequency dependent conductivity measured in microwave absorption experiments shows resonances between $1/5$ and $2/9$ [11], which continue in the insulator below $1/5$ until $\nu = 0.18$. It is tempting to attribute these features to the ^{2}CFC on either side of the $1/5$ state. A qualitative change in the behavior and a decreasing pinning frequency below $\nu = 0.18$ may indicate a transition into a ^{4}CFC, although further work will be needed for a conclusive statement. We note that, unlike for MZ or LG crystals, the pinning frequency of the CFC is predicted to have a complicated dependence on ν and can sometimes decrease with increasing ν in the regime $r_f > \ell$; such behaviors have been seen in lower mobility samples [6,7]. The transition temperatures obtained above are generally higher than those estimated from experiments (although a clean transition has not yet been observed). We also note that we have not considered disorder and LL mixing, which will affect the phase boundaries and melting temperatures.

A. C. A. and J. K. J. thank the National Science Foundation for support under Grant No. DMR-1005536 and the Research Computing and Cyberinfrastructure, a unit of Information and Technology Services at Pennsylvania State University,

for providing high-performance computing resources. K. P. thanks the National Research Foundation of Korea (NRF) funded by the Korea government (MSIP) under Quantum Metamaterials Research Center Grant No. 2008-0062238.

[1] E. Wigner, Phys. Rev. **46**, 1002 (1934).
[2] Y. E. Lozovik and V. I. Yudson, JETP Lett. **22**, 11 (1975).
[3] H. W. Jiang, R. L. Willett, H. L. Stormer, D. C. Tsui, L. N. Pfeiffer, and K. W. West, Phys. Rev. Lett. **65**, 633 (1990); H. W. Jiang, H. L. Stormer, D. C. Tsui, L. N. Pfeiffer, and K. W. West, Phys. Rev. B **44**, 8107 (1991).
[4] V. J. Goldman, M. Santos, M. Shayegan, and J. E. Cunningham, Phys. Rev. Lett. **65**, 2189 (1990).
[5] W. Pan, H. L. Stormer, D. C. Tsui, L. N. Pfeiffer, K. W. Baldwin, and K. W. West, Phys. Rev. Lett. **88**, 176802 (2002).
[6] L. W. Engel, C.-C. Li, D. Shahar, D. C. Tsui, and M. Shayegan, Physica (Amsterdam) **1E**, 111 (1997).
[7] C. C. Li, J. Yoon, L. W. Engel, D. Shahar, D. C. Tsui, and M. Shayegan, Phys. Rev. B **61**, 10 905 (2000).
[8] P. D. Ye, L. W. Engel, D. C. Tsui, R. M. Lewis, L. N. Pfeiffer, and K. West, Phys. Rev. Lett. **89**, 176802 (2002).
[9] Y. P. Chen, R. M. Lewis, L. W. Engel, D. C. Tsui, P. D. Ye, Z. H. Wang, L. N. Pfeiffer, and K. W. West, Phys. Rev. Lett. **93**, 206805 (2004).
[10] G. Sambandamurthy, Z. Wang, R. M. Lewis, Y. P. Chen, L. W. Engel, D. C. Tsui, L. N. Pfeiffer, and K. W. West, Solid State Commun. **140**, 100 (2006), and references contained therein.
[11] Y. P. Chen, G. Sambandamurthy, Z. H. Wang, R. M. Lewis, L. W. Engel, D. C. Tsui, P. D. Ye, L. N. Pfeiffer, and K. W. West, Nat. Phys. **2**, 452 (2006).
[12] D. C. Tsui, H. L. Stormer, and A. C. Gossard, Phys. Rev. Lett. **48**, 1559 (1982).
[13] K. Maki and X. Zotos, Phys. Rev. B **28**, 4349 (1983).
[14] P. K. Lam and S. M. Girvin, Phys. Rev. B **30**, 473 (1984).
[15] D. Levesque, J. J. Weis, and A. H. MacDonald, Phys. Rev. B **30**, 1056 (1984).
[16] K. Esfarjani and S. T. Chui, Phys. Rev. B **42**, 10 758 (1990).
[17] R. Côté and A. H. MacDonald, Phys. Rev. B **44**, 8759 (1991).
[18] H. Yi and H. A. Fertig, Phys. Rev. B **58**, 4019 (1998).
[19] R. Narevich, G. Murthy, and H. A. Fertig, Phys. Rev. B **64**, 245326 (2001).
[20] K. Yang, F. D. M. Haldane, and E. H. Rezayi, Phys. Rev. B **64**, 081301 (2001).
[21] N. Shibata and D. Yoshioka, J. Phys. Soc. Jpn. **72**, 664 (2003).
[22] S. S. Mandal, M. R. Peterson, and J. K. Jain, Phys. Rev. Lett. **90**, 106403 (2003).
[23] G. S. Jeon, C. C. Chang, and J. K. Jain, J. Phys. Condens. Matter **16**, L271 (2004); Phys. Rev. B **69**, 241304(R) (2004).
[24] C.-C. Chang, G. S. Jeon, and J. K. Jain, Phys. Rev. Lett. **94**, 016809 (2005).
[25] W. J. He, T. Cui, Y. M. Ma, C. B. Chen, Z. M. Liu, and G. T. Zou, Phys. Rev. B **72**, 195306 (2005).
[26] C.-C. Chang, C. Töke, G. S. Jeon, and J. K. Jain, Phys. Rev. B **73**, 155323 (2006).
[27] C. Shi, G. S. Jeon, and J. K. Jain, Phys. Rev. B **75**, 165302 (2007).
[28] J. K. Jain and R. K. Kamilla, Int. J. Mod. Phys. B **11**, 2621 (1997); Phys. Rev. B **55**, R4895 (1997).
[29] R. B. Laughlin, Phys. Rev. Lett. **50**, 1395 (1983).
[30] J. K. Jain, Phys. Rev. Lett. **63**, 199 (1989); Phys. Rev. B **41**, 7653 (1990); Phys. Today **53**, 39 (2000).
[31] J. K. Jain, *Composite Fermions* (Cambridge University Press, Cambridge, England, 2007).
[32] H. Zhu, Y. P. Chen, P. Jiang, L. W. Engel, D. C. Tsui, L. N. Pfeiffer, and K. W. West, Phys. Rev. Lett. **105**, 126803 (2010).
[33] F. D. M. Haldane, Phys. Rev. Lett. **51**, 605 (1983).
[34] J. Thomson, Philos. Mag. **7**, 237 (1904).
[35] D. J. Wales and S. Ulker, Phys. Rev. B **74**, 212101 (2006); D. J. Wales, H. McKay, and E. L. Altschuler, *ibid.* **79**, 224115 (2009). The minimum energy locations can be found at http://thomson.phy.syr.edu/.
[36] M. Greiter, Phys. Rev. B **83**, 115129 (2011).
[37] T. D. Rhone, L. Tiemann, and K. Muraki (unpublished).
[38] See Supplemental Material at http://link.aps.org/supplemental/10.1103/PhysRevLett.111.146804 for the N dependence of the phase boundary, details of our curve fittings, the parameters used in estimating the melting temperature, and density distributions of various CFCs.
[39] X. G. Wu, G. Dev, and J. K. Jain, Phys. Rev. Lett. **71**, 153 (1993).
[40] C. Shi, S. Jolad, N. Regnault, and J. K. Jain, Phys. Rev. B **77**, 155127 (2008).
[41] H. Buhmann, W. Joss, K. von Klitzing, I. V. Kukushkin, G. Martinez, A. S. Plaut, K. Ploog, and V. B. Timofeev, Phys. Rev. Lett. **65**, 1056 (1990); H. Buhmann, W. Joss, K. von Klitzing, I. V. Kukushkin, A. S. Plaut, G. Martinez, K. Ploog, and V. B. Timofeev, Phys. Rev. Lett. **66**, 926 (1991).
[42] M. Hayne, M. K. Ellis, A. S. Plaut, A. Usher, and K. Ploog, Surf. Sci. **263**, 39 (1992).
[43] E. M. Goldys, S. A. Brown, R. B. Dunford, A. G. Davies, R. Newbury, R. G. Clark, P. E. Simmonds, J. J. Harris, and C. T. Foxon, Phys. Rev. B **46**, 7957 (1992).
[44] J. M. Kosterlitz and D. J. Thouless, J. Phys. C **6**, 1181 (1973).
[45] D. J. Thouless and M. E. Elzain, J. Phys. C: Solid State Phys. **11**, 3425 (1978).
[46] P. M. Platzman and R. Price, Phys. Rev. Lett. **70**, 3487 (1993); R. Price, X. Zhu, P. M. Platzman, and S. G. Louie, Phys. Rev. B **48**, 11 473 (1993).
[47] R. Chitra, T. Giamarchi, and P. Le Doussal, Phys. Rev. Lett. **80**, 3827 (1998).
[48] R. Chitra, T. Giamarchi, and P. Le Doussal, Phys. Rev. B **65**, 035312 (2001).